Economic Modelling 69 (2018) 291–300

Contents lists available at ScienceDirect

Economic Modelling

journal homepage: www.elsevier.com/locate/econmod

The Great Recession and Okun's law

Angelia L. Grant[1]

Economics Discipline Group, University of Technology Sydney, PO Box 123, Broadway NSW 2007, Australia

ARTICLE INFO

JEL classification:
C11
C15
C52
C58

Keywords:
Time variation
Output gap
Unemployment gap

ABSTRACT

The relationship between output and unemployment has been a widely discussed topic since the Great Recession. This paper jointly estimates a time-varying parameter Okun's law with two latent states: potential output and the natural rate of unemployment. It is found that there is substantial time variation in the Okun's coefficient in the US. Since the Great Recession, a given unemployment gap has been associated with a smaller output gap. The probability that the Okun's coefficient is equal to the widely accepted value of −2 fell significantly during the Great Recession, but has since risen despite the Okun's coefficient remaining at around −0.5. This illustrates the significant degree of uncertainty in the estimation of potential output and the natural rate of unemployment.

1. Introduction

The relationship between output and unemployment has been a widely discussed topic since the Great Recession. The literature has examined the pattern of jobless recoveries, changes in the persistence of the unemployment rate and the difference between labor market outcomes in financial recessions versus other recessions (see, e.g., Stock and Watson, 2012; Basu and Foley, 2013; Boeri et al., 2013; Calvo et al., 2013; Valadkhani and Smyth, 2015; Hall, 2017; Marques et al., 2017).

This paper aims to add further to this empirical literature. More specifically, it examines whether Okun's law—the empirical relationship between unemployment and output that was first observed by Okun (1962)—still holds. To do this, it estimates a time-varying gap version of Okun's law, which allows for stochastic volatility in the output gap equation. In addition, formal inference is conducted to determine whether the Okun's coefficient is statistically different from the traditional estimate of −2. This is important given parameter uncertainty, but is not usually done in the literature.

The gap version of Okun's law relates the output gap to the unemployment gap, where the output gap is the difference between actual and potential log output and the unemployment gap is the difference between the actual and natural rate of unemployment. In contrast, the difference version of Okun's law postulates a linear relationship between the first difference of the log of output and the first difference of the unemployment rate. While the difference version is easier to estimate, the gap version has the advantage of taking into account the state of the economy compared with its trend or natural state. In fact, the gap version is a more general version of the relationship in difference terms (see, e.g., Guisinger et al., 2015). The gap version collapses to the difference version if it is assumed that potential growth and the natural rate of unemployment are constant. Given that there are a number of reasons to expect that this would not be the case, the gap version would appear to be a better estimation choice than the difference version.

There are also many reasons why the relationship between unemployment and output would not be constant. Most notably, it would be reasonable to expect structural changes over time in productivity and the labor market. A number of researchers have examined structural instability in the Okun's coefficient using a variety of estimation techniques. Some focus on structural breaks (see, e.g., Weber, 1995; Lee, 2000; Galí et al., 2012; Ball et al., 2013), some focus on general time variation (see, e.g., Sögner and Stiassny, 2002; Huang and Lin, 2008; Beaton, 2010), and others focus on whether the relationship is asymmetric over the business cycle (see, e.g., Cuaresma, 2003; Silvapulle et al., 2004; Holmes and Silverstone, 2006; Wang and Huang, 2017). However, most of the literature focuses on the difference version rather than the gap version of Okun's law.

The smaller number of papers that focus on time variation in the gap version of Okun's law tend to consider only a restricted form of time variation. They also generally use two-stage estimation procedures, where the estimates of potential output and the natural rate of unemployment are obtained from filters or modeled using a deterministic trend. The exceptions are Huang and Lin (2008) who propose a smooth time-varying parameter approach that allows the coefficients to shift in a non-parametric but smooth way, Valadkhani and Smyth

E-mail address: angelia.l.grant@gmail.com.

[1] I would like to thank Joshua Chan for helpful comments.

http://dx.doi.org/10.1016/j.econmod.2017.10.002
Received 1 June 2017; Received in revised form 27 August 2017; Accepted 2 October 2017
Available online 21 October 2017
0264-9993/

(2015) who use a Markov switching model that allows for asymmetries within and across regimes, and Berger et al. (2016) who estimate a multivariate unobserved components model with time-varying parameters and stochastic volatility.

A time-varying parameter model is a less restricted form of time variation than considering specific structural breaks or using rolling regressions. In addition, the estimation allows for the joint estimation of potential output, the natural rate of unemployment and the model parameters, in contrast to a two-stage estimation procedure where the latent variables are either obtained from filters or modeled using a deterministic trend. This improves efficiency and avoids the problem of attenuation bias. It is particularly preferable to the use of filters, which suffer from attenuation bias and can generate spurious cycles (see, e.g., King and Rebelo, 1993; Cogley and Nason, 1995; Canova, 1998). Further, given the empirical relevance of time-varying volatility in macroeconomic variables, the estimation allows for stochastic volatility in the output gap equation. The modeling framework is closest to Chan et al. (2016) and Berger et al. (2016). However, the former focuses on forecasting inflation, while the latter focuses on testing time variation against time-invariant specifications rather than testing the value of the Okun's coefficient.

The estimation of a time-varying gap version of Okun's law shows substantial time variation in the Okun's coefficient in the US, with rises in the coefficient often experienced during recessions. Before 1980 the coefficient fluctuates between −2.5 and −2, which is close to the widely accepted value of −2. After this it increases substantially and fluctuates between −1.5 and −1 before the onset of the Great Recession. During the Great Recession the coefficient increases substantially and makes further gains following the worst of the recession. The coefficient is estimated to most recently be around −0.5, which is only one-quarter of the widely accepted value of the coefficient. This means that a given unemployment gap has been associated with a smaller output gap over the sample period of 1948Q1 to 2016Q4. While some of the shift in the Okun's coefficient may be reversed as the effects of the Great Recession continue to recede, a significant proportion of the increase in the coefficient occurred before the onset of the Great Recession. This may indicate that a structural shift in the relationship was already underway, possibly as a result of structural shifts in the labor market or productivity.

However, parameter uncertainty around the Okun's coefficient means that the estimated coefficient might not be statistically different from the traditional estimate of −2. This is formally tested by computing the dynamic probabilities that the Okun's coefficient is equal to −2 using the methodology in Koop et al. (2010). It is found that before the Great Recession the Okun's coefficient is equal to −2 with high probability despite the parameter estimate having increased substantially. The probability that the coefficient is equal to −2 then falls substantially as a result of the Great Recession, but has since risen despite the coefficient remaining at around −0.5.

The remainder of this paper is organized as follows. Section 2 outlines the bivariate unobserved components model used for the analysis. Section 3 describes the data and presents the empirical results. Section 4 concludes.

2. Bivariate unobserved components model

This section introduces the bivariate unobserved components model with time-varying parameters and stochastic volatility, similar to that in Chan et al. (2016). More specifically, consider the following bivariate model for (log) output, y_t, and the unemployment rate, u_t:

$$(y_t - y_t^*) = \lambda_t(u_t - u_t^*) + \varepsilon_t^y, \tag{1}$$

$$(u_t - u_t^*) = \varepsilon_t^u, \tag{2}$$

where y_t^* and u_t^* are potential output and the natural rate of unemployment respectively.

Eq. (1) is based on one of the empirical relationships specified by Okun (1962). More specifically, this is the gap version of Okun's law where the deviation of output from its potential, $y_t - y_t^*$, depends on the deviation of the unemployment rate from its natural rate, $u_t - u_t^*$. For example, when the unemployment rate is equal to its natural rate, output equals its trend or potential on average. When there is an increase in the unemployment gap, real output will be below its potential. In contrast to the original specification in Okun (1962), the relationship between the output gap and the unemployment gap is time-varying. In addition, it is assumed that the variance of the transitory component is time-varying via a stochastic volatility process, i.e., $\varepsilon_t^y \sim \mathcal{N}(0, e^{h_t})$.

The deviation of the unemployment rate from its natural rate is assumed to follow an AR(2) process:

$$\varepsilon_t^u = \rho_1\varepsilon_{t-1}^u + \rho_2\varepsilon_{t-2}^u + \eta_t, \tag{3}$$

where $\eta_t \sim \mathcal{N}(0, \sigma_u^2)$ and $\varepsilon_0^u = \varepsilon_{-1}^u = 0$. The unemployment gap is modeled as a stationary AR(2) process to ensure that the typically high persistence in the unemployment gap is taken into account. The time-varying parameter and stochastic volatility process evolve according to the following random walk processes:

$$\lambda_t = \lambda_{t-1} + \varepsilon_t^\lambda, \tag{4}$$

$$h_t = h_{t-1} + \varepsilon_t^h, \tag{5}$$

where ε_t^λ and ε_t^h are independent $\mathcal{N}(0, \sigma_\lambda^2)$ and $\mathcal{N}(0, \sigma_h^2)$ respectively. These state equations are initialized with $\lambda_1 \sim \mathcal{N}(\lambda_0, V_\lambda)$ and $h_1 \sim \mathcal{N}(h_0, V_h)$.[2]

Potential output and the natural rate of unemployment also follow random walk processes:

$$y_t^* = \gamma + y_{t-1}^* + \varepsilon_t^{y*}, \tag{6}$$

$$u_t^* = u_{t-1}^* + \varepsilon_t^{u*}, \tag{7}$$

where ε_t^{y*} and ε_t^{u*} are independent $\mathcal{N}(0, \sigma_{y*}^2)$ and $\mathcal{N}(0, \sigma_{u*}^2)$ respectively, and the processes are initialized with $y_1^* \sim \mathcal{N}(y_0^*, V_{y*})$ and $u_1^* \sim \mathcal{N}(u_0^*, V_{u*})$.[3,4]

2.1. Priors

The following independent prior distributions are assumed for the model parameters:

$$\boldsymbol{\rho} \sim \mathcal{N}(\boldsymbol{\rho}_0, \mathbf{V}_\rho), \quad \gamma \sim \mathcal{N}(\gamma_0, V_\gamma), \quad \sigma_\lambda^2 \sim \mathcal{IG}(\nu_\lambda, S_\lambda), \quad \sigma_h^2 \sim \mathcal{IG}(\nu_h, S_h),$$

$$\sigma_{y*}^2 \sim \mathcal{IG}(\nu_{y*}, S_{y*}), \quad \sigma_{u*}^2 \sim \mathcal{IG}(\nu_{u*}, S_{u*}), \quad \sigma_u^2 \sim \mathcal{IG}(\nu_u, S_u),$$

where $\boldsymbol{\rho} = (\rho_1, \rho_2)'$ and $\mathcal{IG}(\cdot, \cdot)$ denotes the inverse-gamma distribution. More specifically, the following proper, but relatively noninformative hyperparameters, are chosen: $\boldsymbol{\rho}_0 = (0.8\ 0.1)'$, $\mathbf{V}_\rho = \text{diag}(1, 1)$, $\gamma_0 = 0$, $V_\gamma = 5$, $\nu_\lambda = \nu_h = \nu_{y*} = \nu_{u*} = \nu_u = 5$, $S_\lambda = S_h = 0.04$, $S_{y*} = S_{u*} = 0.4$ and $S_u = 1$. These priors give: $E(\sigma_\lambda^2) = E(\sigma_h^2) = 0.01$, $E(\sigma_{y*}^2) = E(\sigma_{u*}^2) = 0.1$ and $E(\sigma_u^2) = 0.25$. The prior mean for $\boldsymbol{\rho}$ is set based on the belief that the unemployment gap is persistent and stationary, while the other priors have been set similar to those in the literature (see, e.g., Chan et al., 2016).

[2] The inclusion of stochastic volatility in the measurement equation for output is important given the pioneering work of Cogley and Sargent (2005); Primiceri (2005) and Sims and Zha (2006). It is less common, however, for the literature to account for stochastic volatility in the unemployment rate (see, e.g. Chan et al., 2016).

[3] This model is a standard bivariate unobserved components model and identification is achieved without the need for restricting the variances: u_t^* is identified by Eqs. (2) and (3) so Eq. (1) becomes a time-varying parameter model with a time-varying intercept (y_t^*) and a time-varying parameter (λ_t).

[4] This specification is similar to that in Berger et al. (2016), but they regress the unemployment gap on the output gap. Due to different specifications, there are notable differences in the timing and magnitude of the changes in the Okun's coefficient.

2.2. Estimation

This section outlines the Bayesian estimation method used to fit the model. A key feature of the estimation is that it draws on recent advances in band matrix algorithms developed in Chan and Jeliazkov, 2009 and McCausland et al., 2011, which are shown to be more efficient than the conventional Kalman filter-based algorithms. In particular, a Gibbs sampler is used to simulate from the posterior distribution. For notational convenience, let $\mathbf{y} = (y_1, \ldots, y_T)'$, $\mathbf{y}^* = (y_1^*, \ldots, y_T^*)'$, $\boldsymbol{\Lambda} = \mathrm{diag}(\lambda_1, \ldots, \lambda_T)$, $\boldsymbol{\lambda} = (\lambda_1, \ldots, \lambda_T)'$, $\mathbf{u} = (u_1, \ldots, u_T)'$, $\mathbf{u}^* = (u_1^*, \ldots, u_T^*)'$, $\mathbf{h} = (\mathbf{h}_1, \ldots, \mathbf{h}_T)'$.

The posterior draws can be obtained by sequentially sampling from the following conditional distributions: (1) $p(\mathbf{y}^* \mid \mathbf{y}, \mathbf{u}, \mathbf{u}^*, \boldsymbol{\Lambda}, \mathbf{h}, \sigma_{y*}^2)$; (2) $p(\mathbf{u}^* \mid \mathbf{y}, \mathbf{y}^*, \mathbf{u}, \boldsymbol{\Lambda}, \mathbf{h}, \boldsymbol{\rho}, \sigma_u^2, \sigma_{u*}^2)$; (3) $p(\gamma \mid \mathbf{y}^*, \sigma_{y*}^2)$; (4) $p(\lambda \mid \mathbf{y}, \mathbf{y}^*, \mathbf{u}, \mathbf{u}^*, \mathbf{h}, \sigma_\lambda^2)$; (5) $p(\mathbf{h} \mid \mathbf{y}, \mathbf{y}^*, \mathbf{u}, \mathbf{u}^*, \lambda, \sigma_h^2)$; (6) $p(\boldsymbol{\rho} \mid \mathbf{u}, \mathbf{u}^*, \sigma_u^2)$; (7) $p(\sigma_u^2 \mid \mathbf{u}, \mathbf{u}^*, \boldsymbol{\rho})$; (8) $p(\sigma_\lambda^2 \mid \lambda)$; (9) $p(\sigma_h^2 \mid \mathbf{h})$; (10) $p(\sigma_{y*}^2 \mid \mathbf{y}^*)$; (11) $p(\sigma_{u*}^2 \mid \mathbf{u}^*)$.

The sampling step for drawing the latent states for potential output is briefly discussed, with the technical details of the other steps outlined in the Appendix.[5]

To implement Step 1, first stack the measurement Eq. (1) over t as follows:

$$\mathbf{y} = \mathbf{y}^* + \boldsymbol{\Lambda}(\mathbf{u} - \mathbf{u}^*) + \boldsymbol{\epsilon}^{\mathbf{y}}, \tag{8}$$

where $\boldsymbol{\epsilon}^{\mathbf{y}} \sim \mathcal{N}(\mathbf{0}, \boldsymbol{\Sigma})$ and $\boldsymbol{\Sigma} = \mathrm{diag}(\mathrm{e}^{h_1}, \ldots, \mathrm{e}^{h_T})$.

It follows that $(\mathbf{y} \mid \mathbf{y}^*, \mathbf{u}, \mathbf{u}^*, \boldsymbol{\Lambda}, \mathbf{h}) \sim \mathcal{N}(\mathbf{y}^* + \boldsymbol{\Lambda}(\mathbf{u} - \mathbf{u}^*), \boldsymbol{\Sigma})$ and hence the log sampling density is given by:

$$\log p(\mathbf{y} \mid \mathbf{y}^*, \mathbf{u}, \mathbf{u}^*, \boldsymbol{\Lambda}, \mathbf{h}) \propto -\frac{1}{2}\sum_{t=1}^{T} h_t - \frac{1}{2}(\mathbf{y} - \mathbf{y}^* - \boldsymbol{\Lambda}(\mathbf{u} - \mathbf{u}^*))' \boldsymbol{\Sigma}^{-1}(\mathbf{y} - \mathbf{y}^* - \boldsymbol{\Lambda}(\mathbf{u} - \mathbf{u}^*)). \tag{9}$$

Next, let $\mathbf{H}$ denote the first difference matrix, i.e.,

$$\mathbf{H} = \begin{pmatrix} 1 & 0 & \cdots & 0 \\ -1 & 1 & \ddots & \vdots \\ \vdots & \ddots & \ddots & \vdots \\ 0 & \cdots & -1 & 1 \end{pmatrix}.$$

Then, the transition equation for y_t^* (6) can be rewritten as:

$$\mathbf{H}\mathbf{y}^* = \tilde{\boldsymbol{\alpha}}_{\mathbf{y}*} + \boldsymbol{\epsilon}^{\mathbf{y}*}, \tag{10}$$

where $\tilde{\boldsymbol{\alpha}}_{\mathbf{y}*} = (y_0^* + \gamma, \gamma, \ldots, \gamma)'$, $\boldsymbol{\epsilon}^{\mathbf{y}*} \sim \mathcal{N}(\mathbf{0}, \boldsymbol{\Omega}_{\mathbf{y}*})$ and $\boldsymbol{\Omega}_{\mathbf{y}*} = \mathrm{diag}(V_{y*}, \sigma_{y*}^2, \ldots, \sigma_{y*}^2)$.

It follows that $(\mathbf{y}^* \mid \sigma_{y*}^2) \sim \mathcal{N}(\boldsymbol{\alpha}_{\mathbf{y}*}, (\mathbf{H}'\boldsymbol{\Omega}_{\mathbf{y}*}^{-1}\mathbf{H})^{-1})$, where $\boldsymbol{\alpha}_{\mathbf{y}*} = \mathbf{H}^{-1}\tilde{\boldsymbol{\alpha}}_{\mathbf{y}*}$. Therefore, the log sampling density is:

$$\log p(\mathbf{y}^* \mid \sigma_{y*}^2) \propto -\frac{1}{2}\log(V_{y*}) - \frac{T-1}{2}\log(\sigma_{y*}^2) - \frac{1}{2}(\mathbf{y}^* - \boldsymbol{\alpha}_{\mathbf{y}*})'\mathbf{H}' \boldsymbol{\Omega}_{\mathbf{y}*}^{-1}\mathbf{H}(\mathbf{y}^* - \boldsymbol{\alpha}_{\mathbf{y}*}). \tag{11}$$

The conditional distribution $p(\mathbf{y}^* \mid \mathbf{y}, \mathbf{u}, \mathbf{u}^*, \boldsymbol{\Lambda}, \mathbf{h}, \sigma_{y*}^2)$ can then be determined using Eqs. (9) and (11):

$$\begin{aligned} &\log p(\mathbf{y}^* \mid \mathbf{y}, \mathbf{u}, \mathbf{u}^*, \boldsymbol{\Lambda}, \mathbf{h}, \sigma_{y*}^2) \\ &\quad \propto \log p(\mathbf{y} \mid \mathbf{y}^*, \mathbf{u}, \mathbf{u}^*, \boldsymbol{\Lambda}, \mathbf{h}) + \log p(\mathbf{y}^* \mid \sigma_{y*}^2) \\ &\quad \propto -\frac{1}{2}(\mathbf{y}^{*\prime}(\boldsymbol{\Sigma}^{-1} + \mathbf{H}'\boldsymbol{\Omega}_{\mathbf{y}*}^{-1}\mathbf{H})\mathbf{y}^* - 2\mathbf{y}^{*\prime}(\boldsymbol{\Sigma}^{-1}(\mathbf{y} - \boldsymbol{\Lambda}(\mathbf{u} - \mathbf{u}^*)) + \mathbf{H}' \\ &\quad \boldsymbol{\Omega}_{\mathbf{y}*}^{-1}\mathbf{H}\boldsymbol{\alpha}_{\mathbf{y}*})). \end{aligned}$$

Therefore, $(\mathbf{y}^* \mid \mathbf{y}, \mathbf{u}, \mathbf{u}^*, \boldsymbol{\Lambda}, \mathbf{h}, \sigma_{y*}^2) \sim \mathcal{N}(\hat{\mathbf{y}}^*, \mathbf{D}_{\mathbf{y}*})$, where

$$\mathbf{D}_{\mathbf{y}*} = (\boldsymbol{\Sigma}^{-1} + \mathbf{H}'\boldsymbol{\Omega}_{\mathbf{y}*}^{-1}\mathbf{H})^{-1}, \quad \hat{\mathbf{y}}^* = \mathbf{D}_{\mathbf{y}*}(\boldsymbol{\Sigma}^{-1}(\mathbf{y} - \boldsymbol{\Lambda}(\mathbf{u} - \mathbf{u}^*)) + \mathbf{H}'\boldsymbol{\Omega}_{\mathbf{y}*}^{-1}\mathbf{H}\boldsymbol{\alpha}_{\mathbf{y}*}).$$

Given that $\boldsymbol{\Sigma}$, $\mathbf{H}$, and $\boldsymbol{\Omega}_{\mathbf{y}*}$ are all band matrices, the precision-based algorithm in Chan and Jeliazkov (2009) can be used to sample $\mathbf{y}^*$ efficiently. The details of the remaining estimation steps are given in the Appendix.

[5] The model is written in different state space forms for different steps in the estimation process depending on which conditional distribution is being drawn from.

3. Results

3.1. Data

The data used are the log of US output and the unemployment rate. Quarterly data on output and the unemployment rate are sourced from the Federal Reserve Bank of St. Louis database. The output series is seasonally adjusted annualized real GDP, while the unemployment rate is the seasonally adjusted civilian unemployment rate. The sample period is 1948Q1 to 2016Q4.

3.2. Output and unemployment gaps

The estimates of potential output, the natural rate of unemployment, and the output and unemployment gaps are shown in Fig. 1. The estimation is based on 50,000 draws, with a burn-in period of 10,000 draws.

The estimates of the output gap are reasonably persistent and align with the National Bureau of Economic Research (NBER) recession dates. The negative output gaps are generally 'deeper' than positive output gaps. This finding has led a number of researchers to explore whether Okun's law is asymmetric over the business cycle (see, e.g., Cuaresma, 2003; Silvapulle et al., 2004; Holmes and Silverstone, 2006; Wang and Huang, 2017).

It is evident from the estimates that the recession from 1981Q3 to 1982Q4 was the deepest recession recorded over this sample period and the 2001 recession was the mildest. In fact, the 2001 recession appears to be a 'correction' following the build-up of a positive output gap in the preceding period. While the Great Recession is not the deepest recession experienced in the US economy since 1948Q1, the recovery following the downturn is noticeably lacking the sharp bounce-back that was experienced in other recessions.

There is also significant time variation in the natural rate of unemployment. It is estimated to have drifted up over the first 30 years of the sample period, before declining from around 7 per cent to 5.8 per cent. It then drifts upwards again from the late 1990s and peaks at almost 7 per cent following the Great Recession. The natural rate of unemployment is estimated to have fallen more recently to 5.9 per cent at the end of the sample period.

The unemployment gap rises sharply in each of the negative output gap periods. However, unlike the output gap, the estimate of the unemployment gap does not exhibit a significant difference in the deepness of recessions and expansions. There appears to be a strong negative correlation between the two gaps, as predicted by Okun's law. The correlation coefficient for the two estimated gaps across the full sample period is −0.9.

However, the relationship between the output and unemployment gaps also seems to be time-varying. In the recessions experienced before the early 1990s, the size of the output gap is generally larger than the size of the unemployment gap. However, the gaps are much closer in magnitude during the recessions in the early 1990s, 2001 and in the Great Recession. This indicates that, more recently, a given unemployment gap has been associated with a smaller output gap. The next section examines whether the formal estimates of time-variation indicate a shift in the relationship.

3.3. Time-varying coefficients and stochastic volatility

The posterior distribution for the Okun's coefficient is shown in Fig. 2(a). The prior distribution of −2, which is the widely accepted value of the coefficient, is also highlighted.

There is substantial time variation in the Okun's coefficient. It fluctuates between −2.5 and −2 before the 1980s. It then rises

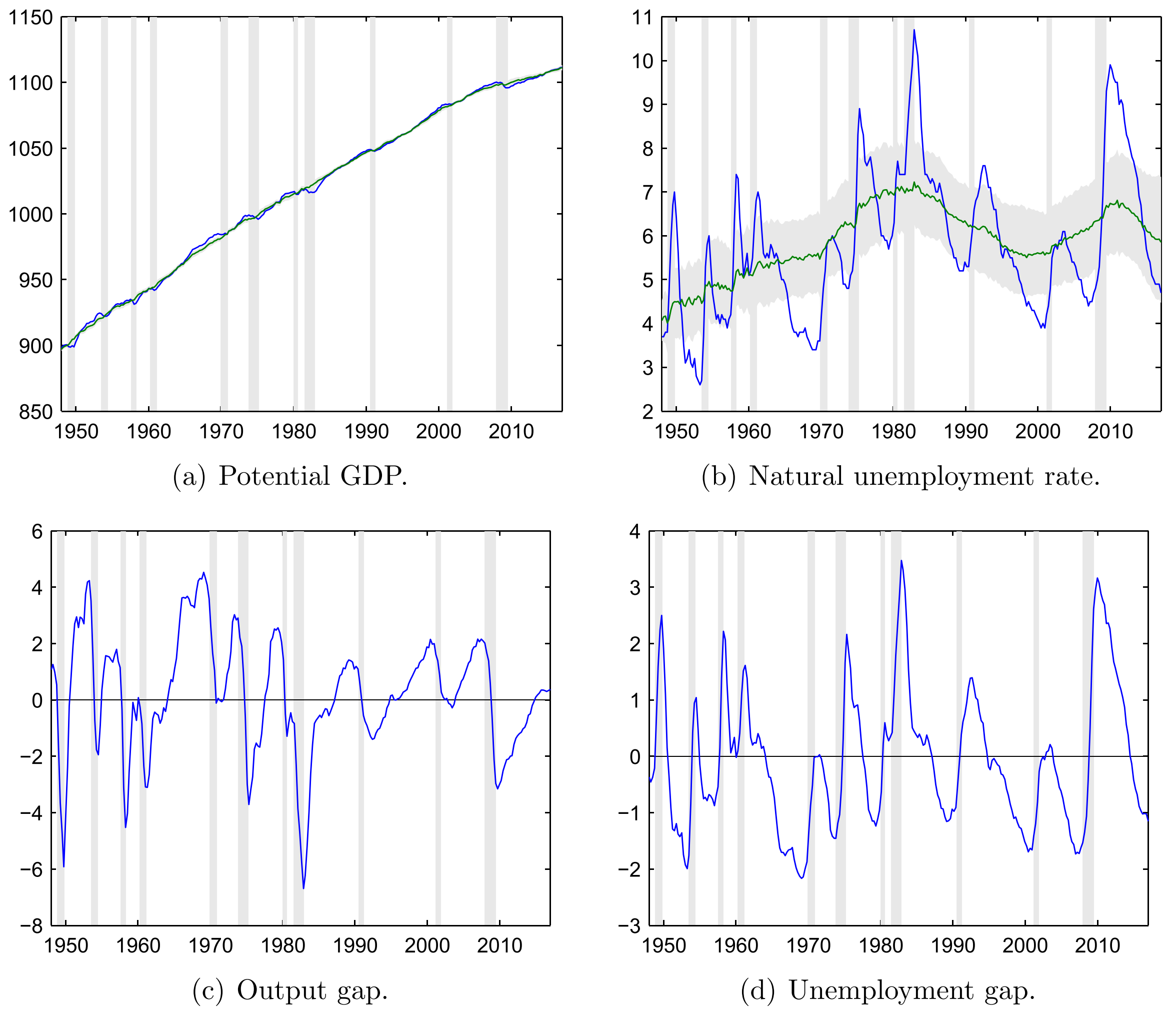

Fig. 1. Estimated output and unemployment gaps.

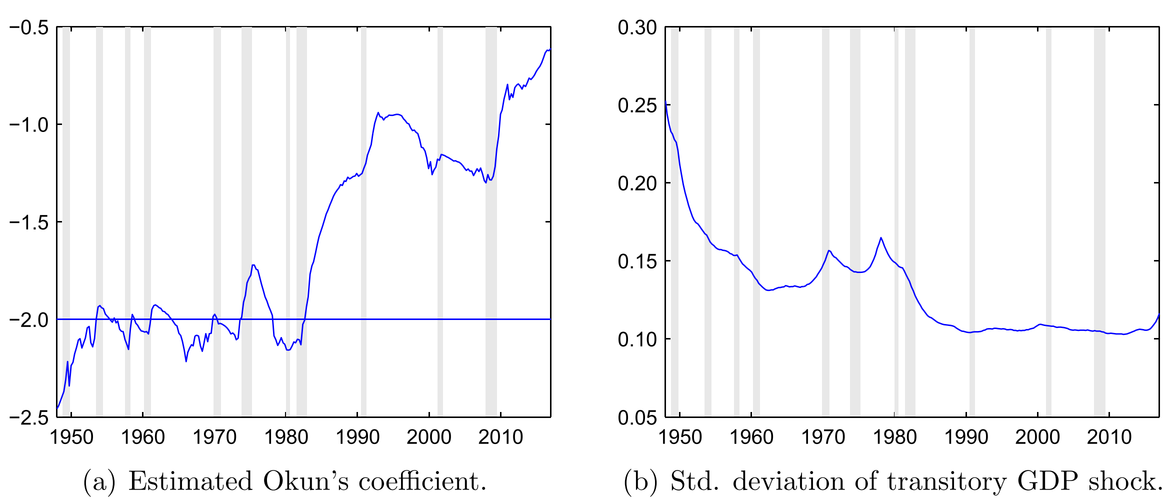

Fig. 2. Time-varying coefficient and stochastic volatility.

substantially and fluctuates between −1.5 and 1 before the onset of the Great Recession. During the Great Recession the coefficient again increases substantially and makes further gains following the worst of the recession. The coefficient is estimated to most recently be around −0.5, which is only one-quarter of the widely accepted value of the coefficient. This means that a given unemployment gap is now associated with a much smaller output gap. This is in contrast to Berger et al. (2016), who find that the Okun's coefficient has returned back to the historical average.

Fig. 2(a) also shows that the Okun's coefficient often rises during recessions, with the strongest rises experienced during the 1980s recession and the Great Recession. The coefficient continued to rise following the 1980s and 1990s recessions, but then fell in the late-1990s to be only slightly above where it was before the 1990s recession. The coefficient rose strongly during the Great Recession and has continued to rise since.

While some of the shift in the Okun's law relationship may be reversed as the effects of the Great Recession continue to recede, it is interesting that a significant proportion of the increase in the coefficient occurred before the onset of the Great Recession. This may indicate that a structural shift in the relationship was already underway.

The structural shift in the Okun's coefficient is likely to be the result of structural shifts in the labor market or productivity. In the absence of shifts in the labor market (e.g. the size of the labor force and hours worked per employee) or labor productivity, as output rises above its potential, unemployed workers will be drawn into the labor market at a constant rate (see, e.g., Kaufman, 1988; Prachowny, 1993). Gordon (2010) considers that productivity has played an important role in the shift in the relationship, with the procyclical productivity response of Okun's law not being evident since the mid-1980s. Daly et al. (2011) also consider that productivity was an important factor in the shift in the coefficient during 2009 and 2010. However, they consider this to be a cyclical, rather than structural, phenomenon that reflected a reorientation of production activity. Daly et al. (2011) also note that elevated uncertainty may have resulted in a diminishing effect on productivity in 2011 and therefore reduced job creation. Basu and Foley (2013) consider that the growth of services industries may be changing the employment-output dynamics. These industries tend to have a lower responsiveness of employment to output, which could reflect the difficulty in measuring their output, so the measure of real GDP is drifting further from capturing changes in aggregate demand that lead to changes in employment. Also focusing on the labor market, Dixon et al. (2017) find that the share of temporary workers is important for explaining changes in the coefficient. Chinn et al. (2014) state that the recent fall in the labor force participation rate has distorted the unemployment rate as a measure of slack.

The finding of time variation in the Okun's coefficient is consistent with the findings of parameter instability by Moosa (1997); Lee (2000); Sögner and Stiassny (2002); Huang and Lin (2008) and Berger et al. (2016). It is also consistent with the finding by Valadkhani and Smyth (2015) that the Okun's law relationship weakened following the 1980s recession. Basu and Foley (2013) also find that the relationship between output growth and employment weakened since the mid-1980s. Marques et al. (2017) and Cheng et al. (2012) respectively find that the pattern of unemployment persistence has changed since the Great Recession and that hysteresis is found with the Great Recession in the sample.

The finding of time variation in the Okun's coefficient is also consistent with other findings in the literature regarding changes in the structure of the US economy and changes in monetary policy. For example, Boivin and Giannoni (2006) find that changes in the structure of the economy have changed the monetary policy propagation mechanism to reduce the effect of monetary policy shocks in the post-1980 period. Clarida et al. (2000) and Lubik and Schorfheide (2004) find significant changes in the monetary policy reaction function between the pre- and post-1979 periods.

In contrast, Weber (1995) and Sögner (2001) find no evidence of structural breaks and conclude there is a stable linear Okun's relationship. Ball et al. (2013) also conclude that deviations from Okun's law are usually modest in size and short-lived. Ball et al. (2013) assess the gap version of Okun's law using a two-stage estimation approach, with the Hodrick-Prescott filter used for estimating potential output and the natural rate of unemployment. It is worth noting the finding by Zanin and Marra (2012) that there is not a consistent difference in the results across the literature that use filters.

Importantly, the conclusion that the Okun's law relationship has shifted over time takes into account stochastic volatility. That is, the variance of the shock to the transitory GDP component is assumed to be time-varying via a stochastic volatility process. Many recent studies have highlighted the importance of taking into account changes across time in both coefficients and the size of shocks when modeling US macroeconomic outcomes (see, e.g., Cogley and Sargent, 2005; Primiceri, 2005; Sims and Zha, 2006; Arias et al., 2007; Benati and Mumtaz, 2007; Justiniano and Primiceri, 2008; Gambetti et al., 2008; Galí and Gambetti, 2009). The fact that the model accounts for stochastic volatility means the shift in the Okun's coefficient is not explained by changes in the size of shocks.

Fig. 2(b) shows the standard deviation of the innovation of the transitory GDP component. It can be seen that the size of the shocks to the transitory component of GDP fell sharply from the start of the sample period to 1960 and then rose again until around 1980. The size of the shocks then fell by around one-third during the Great Moderation, which is consistent with the general finding in the literature. There has been a slight upward drift in the size of shocks from the late 1990s to the mid-2000s, although the size of shocks remained low in historical terms. The size of shocks increased again after 2010, with the increase being relatively sharp in historical terms.

3.4. Dynamic probabilities

This section undertakes a formal assessment of whether the Okun's coefficient is significantly different from −2 using the approach in Koop et al. (2010). Koop et al. (2010) develop methods for calculating the dynamic posterior probabilities $\mathbb{P}(\lambda_t = -2 \mid \mathbf{y})$ for $t = 1, \ldots, T$ using standard posterior output for state space models and the principal of the Savage-Dickey density ratio.

More specifically, if it is assumed *a priori* that it is equally likely that the restriction holds or not (i.e. $\mathbb{P}(\lambda_t = -2) = \mathbb{P}(\lambda_t \neq -2)$), the posterior odds ratio in favor of the restriction can be computed via the Savage-Dickey density ratio:

$$PO_t = \frac{p(\lambda_t = -2 \mid \mathbf{y})}{p(\lambda_t = -2)},$$

where the numerator is the value of the marginal posterior density of λ_t evaluated at −2 and the denominator is the marginal prior density evaluated at −2. While Koop et al. (2010) use Monte Carlo methods based on the Kalman filter, Chan (2015) shows how a direct method based on band matrix routines can be used instead of the Kalman filter, and this method is used in this paper.

Fig. 3(a) shows the estimated dynamic probabilities. It can be seen that the evidence in favor of the parameter value of −2 is relatively steady through most of the sample period. The probability that the restriction does not hold is below 0.1 in the four decades up to 1990 and increases slightly during the 1990s to between 0.1 and 0.2. However, the probability that the restriction is not supported increases significantly during the Great Recession, peaking at 0.76 in 2010.

These results highlight both the importance of time-varying parameters and the uncertainty in the estimation. While the Okun's coefficient continues to increase after 2010 to most recently be around −0.5, the probability that the restriction is not supported falls reflecting the wide credible intervals (see Fig. 3(b)). The credible intervals contain −2 for most of the sample period and suggest a significant statistical relationship between the output gap and the unemployment gap throughout most of the sample period. It is only since 2010 that the credible intervals include 0.[6]

The rise in the probability that the coefficient is not equal to −2 during the Great Recession and the subsequent fall is consistent with the literature that concludes that it was cyclical factors such as job mismatch and economic uncertainty, rather than structural factors that influenced the Okun's law relationship during the Great Recession (see, e.g., Daly et al., 2011; Lazear and Spletzer, 2012; Farber, 2012; Chen

[6] However, if the dynamic probabilities are estimated to determine the evidence in favor of the parameter value of 0, it shows that the probability that the Okun's coefficient is equal to 0 rose following the 1990s recession to be over 0.8. This probability then fell, reaching just above 0.1 in 2007. It then rose sharply in 2009 to be over 0.6 and was over 0.9 in 2016.

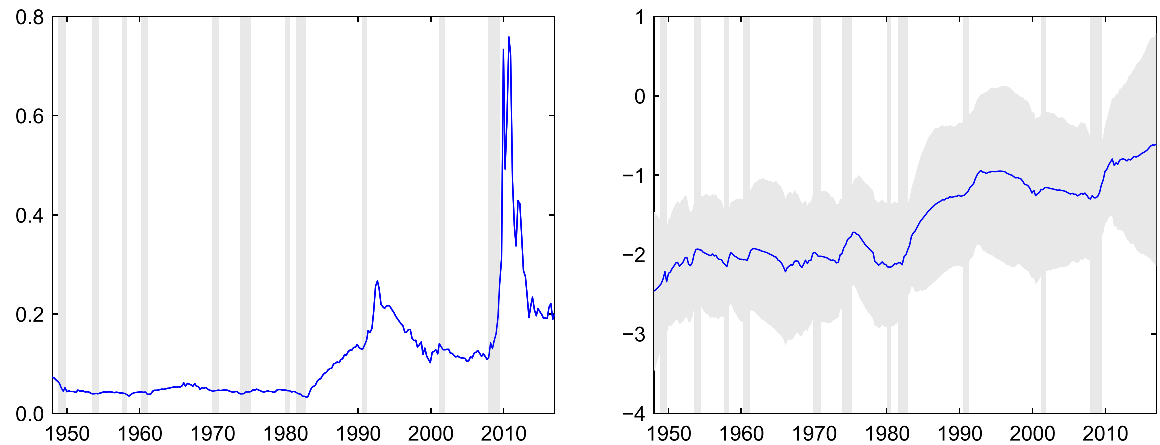

(a) Dynamic posterior probabilities that $\lambda_t \neq -2$.

(b) Okun's coefficient credible intervals.

Fig. 3. Dynamic posterior probabilities and 90% credible intervals.

Table 1
Parameter estimates. Numerical standard errors in parentheses.

ρ_1	ρ_2	σ_u^2	σ_λ^2	σ_h^2	γ	σ_{y*}^2	σ_{u*}^2
1.61 (0.06)	−0.68 (0.06)	0.10 (0.01)	0.03 (0.01)	0.20 (0.06)	0.79 (0.05)	0.73 (0.07)	0.03 (0.01)

et al., 2012).

3.5. Parameter estimates

While the previous sections have reported the time-varying parameters of the bivariate unobserved components model, this section reports the constant coefficient parameter estimates. These parameters are reported in Table 1.

The unemployment gap is strongly persistent, with the sum of the two autoregressive coefficients being significantly different from 0 at 0.93, and the variance of the innovation to the unemployment gap is relatively small at 0.10. The variance of the innovation to the Okun's coefficient is also small at 0.03, while the variance of the innovation to log volatility is somewhat larger at 0.20. The estimate of potential GDP growth is also significantly different from 0 at 0.79, giving an annualized trend growth rate of 3.2 per cent.[7] The variance of the innovation to potential output is 0.73, while the variance of the innovation to the natural rate of unemployment is much smaller at 0.03.

4. Concluding remarks and future research

This paper estimates a time-varying gap version of Okun's law. In contrast to a typical two-stage estimation procedure where the latent variables of potential output and the natural rate of unemployment are either obtained from filters or modeled using a deterministic trend, these variables and the model parameters are estimated jointly. It is found that there is substantial time variation in the Okun's coefficient in the US. The probability that the coefficient is equal to the widely accepted value of −2 fell significantly during the Great Recession, but has since risen despite the Okun's coefficient remaining at around −0.5. This illustrates the significant degree of uncertainty in the estimation of potential output and the natural rate of unemployment.

Future research could focus on multivariate models that include labor supply and labor productivity variables in order to add to the literature on the structural drivers that may be responsible for the change in the coefficient over time.

Appendix: estimation details

This Appendix outlines the estimation details for steps (2) to (11) of the Gibbs sampler outlined in Section 2.2.

To implement Step 2, begin by stacking the state equation for u_t^* (7) over t:

$$\mathbf{H}\mathbf{u}^* = \tilde{\boldsymbol{\alpha}}_{u*} + \boldsymbol{\epsilon}^{\mathbf{u}*}, \tag{12}$$

where $\tilde{\boldsymbol{\alpha}}_{u*} = (u_0^*, 0, \dots, 0)'$, $\boldsymbol{\epsilon}^{\mathbf{u}*} \sim \mathcal{N}(\mathbf{0}, \boldsymbol{\Omega}_{\mathbf{u}*})$ and $\boldsymbol{\Omega}_{\mathbf{u}*} = \text{diag}(V_{u*}, \sigma_{u*}^2, \dots, \sigma_{u*}^2)$.

It follows that $(\mathbf{u}^* \mid \sigma_{u*}^2) \sim \mathcal{N}(\boldsymbol{\alpha}_{\mathbf{u}*}, (\mathbf{H}'\boldsymbol{\Omega}_{\mathbf{u}*}^{-1}\mathbf{H})^{-1})$, where $\boldsymbol{\alpha}_{\mathbf{u}*} = \mathbf{H}^{-1}\tilde{\boldsymbol{\alpha}}_{\mathbf{u}*}$. Therefore, the log sampling density is:

$$\log p(\mathbf{u}^* \mid \sigma_{u*}^2) \propto -\frac{1}{2}\log(V_{u*}) - \frac{T-1}{2}\log(\sigma_{u*}^2) - \frac{1}{2}(\mathbf{u}^* - \boldsymbol{\alpha}_{\mathbf{u}*})'\mathbf{H}'\boldsymbol{\Omega}_{\mathbf{u}*}^{-1}\mathbf{H}(\mathbf{u}^* - \boldsymbol{\alpha}_{\mathbf{u}*}). \tag{13}$$

The next step is to rewrite the AR(2) process for the deviation of the unemployment rate from its natural rate (3) as follows:

$$\mathbf{H}_\rho \boldsymbol{\epsilon}^{\mathbf{u}} = \boldsymbol{\eta}, \tag{14}$$

where $\boldsymbol{\epsilon}^{\mathbf{u}} = (\varepsilon_1^u, \dots, \varepsilon_T^u)'$, $\boldsymbol{\eta} \sim \mathcal{N}(\mathbf{0}, \mathbf{I}_T\sigma_u^2)$ and

[7] The estimate of trend growth is close to that in Hall (2017), which finds trend growth of 3.1 per cent over the sample period of 1948 to 2015. Hall (2017) notes that the trend rate of growth was unusually high around 1950, continued at normal levels until the mid-1960s, had another burst of growth until the late 1960s, continued at normal levels until 2007, and then fell up to 2015.

$$\mathbf{H}_\rho = \begin{pmatrix} 1 & 0 & \cdots & \cdots & 0 \\ -\rho_1 & 1 & \ddots & \vdots & 0 \\ -\rho_2 & -\rho_1 & 1 & \ddots & 0 \\ \vdots & \ddots & \ddots & \ddots & \vdots \\ 0 & \cdots & -\rho_2 & -\rho_1 & 1 \end{pmatrix}.$$

It follows that $(\boldsymbol{\epsilon}^{\mathbf{u}} \mid \boldsymbol{\rho}, \sigma_u^2) \sim \mathcal{N}(\mathbf{0}, \sigma_u^2(\mathbf{H}'_\rho \mathbf{H}_\rho)^{-1})$ and $(\mathbf{u} \mid \mathbf{u}^*, \boldsymbol{\rho}, \sigma_u^2) \sim \mathcal{N}(\mathbf{u}^*, \sigma_u^2(\mathbf{H}'_\rho \mathbf{H}_\rho)^{-1})$. Therefore, the log sampling density is:

$$\log p(\mathbf{u} \mid \mathbf{u}^*, \boldsymbol{\rho}, \sigma_u^2) \propto -\frac{T}{2}\log(\sigma_u^2) - \frac{1}{2\sigma_u^2}(\mathbf{u} - \mathbf{u}^*)'\mathbf{H}'_\rho \mathbf{H}_\rho(\mathbf{u} - \mathbf{u}^*). \tag{15}$$

Eqs. (9), (13) and (15) can be used to determine the conditional distribution:

$$\begin{aligned} &\log p(\mathbf{u}^* \mid \mathbf{y}, \mathbf{y}^*, \mathbf{u}, \boldsymbol{\Lambda}, \mathbf{h}, \boldsymbol{\rho}, \sigma_u^2, \sigma_{u*}^2) \\ &\propto \log p(\mathbf{y} \mid \mathbf{y}^*, \mathbf{u}, \mathbf{u}^*, \boldsymbol{\Lambda}, \mathbf{h}) + \log p(\mathbf{u}^* \mid \sigma_{u*}^2) + \log p(\mathbf{u} \mid \mathbf{u}^*, \boldsymbol{\rho}, \sigma_u^2) \\ &\propto -\frac{1}{2}(\mathbf{u}^{*\prime}(\boldsymbol{\Lambda}'\boldsymbol{\Sigma}^{-1}\boldsymbol{\Lambda} + \mathbf{H}'\boldsymbol{\Omega}_{\mathbf{u}*}^{-1}\mathbf{H} + \mathbf{H}'_\rho \mathbf{H}_\rho/\sigma_u^2)\mathbf{u}^* \\ &\qquad -2\mathbf{u}^{*\prime}(-\boldsymbol{\Lambda}'\boldsymbol{\Sigma}^{-1}(\mathbf{y} - \mathbf{y}^* - \boldsymbol{\Lambda}\mathbf{u}) + \mathbf{H}'\boldsymbol{\Omega}_{\mathbf{u}*}^{-1}\mathbf{H}\boldsymbol{\alpha}_{\mathbf{u}*} + \mathbf{H}'_\rho \mathbf{H}_\rho \mathbf{u}/\sigma_u^2)) \end{aligned}$$

Therefore, $(\mathbf{u}^* \mid \mathbf{y}, \mathbf{y}^*, \mathbf{u}, \boldsymbol{\Lambda}, \mathbf{h}, \boldsymbol{\rho}, \sigma_u^2, \sigma_{u*}^2) \sim \mathcal{N}(\hat{\mathbf{u}}^*, \mathbf{D}_{\mathbf{u}*})$, where

$$\begin{aligned} \mathbf{D}_{\mathbf{u}*} &= (\boldsymbol{\Lambda}'\boldsymbol{\Sigma}^{-1}\boldsymbol{\Lambda} + \mathbf{H}'\boldsymbol{\Omega}_{\mathbf{u}*}^{-1}\mathbf{H} + \mathbf{H}'_\rho \mathbf{H}_\rho/\sigma_u^2)^{-1}, \\ \hat{\mathbf{u}}^* &= \mathbf{D}_{\mathbf{u}*}(-\boldsymbol{\Lambda}'\boldsymbol{\Sigma}^{-1}(\mathbf{y} - \mathbf{y}^* - \boldsymbol{\Lambda}\mathbf{u}) + \mathbf{H}'\boldsymbol{\Omega}_{\mathbf{u}*}^{-1}\mathbf{H}\boldsymbol{\alpha}_{\mathbf{u}*} + \mathbf{H}'_\rho \mathbf{H}_\rho \mathbf{u}/\sigma_u^2). \end{aligned}$$

Given that $\boldsymbol{\Sigma}$, $\mathbf{H}$, $\mathbf{H}_\rho$, and $\boldsymbol{\Omega}_{\mathbf{u}*}$ are all band matrices, the precision-based algorithm in Chan and Jeliazkov (2009) can be used to sample $\mathbf{u}^*$ efficiently.

In the case of Step 3, the transition equation for y_t^* (6) can be rewritten as:

$$\mathbf{W}_{\mathbf{y}*} = \gamma \mathbf{1}_T + \boldsymbol{\epsilon}^{\mathbf{y}*}, \tag{16}$$

where $\mathbf{W}_{\mathbf{y}*} = \mathbf{H}\mathbf{y}^* - \boldsymbol{\delta}_{\mathbf{y}*}$ and $\boldsymbol{\delta}_{\mathbf{y}*} = (y_0^*, 0, \ldots, 0)'$.

It follows that $(\mathbf{W}_{\mathbf{y}*} \mid \mathbf{y}^*, \sigma_{y*}^2) \sim \mathcal{N}(\gamma \mathbf{1}_T, \boldsymbol{\Omega}_{\mathbf{y}*})$ and the log sampling density is given by:

$$\log p(\mathbf{W}_{\mathbf{y}*} \mid \mathbf{y}^*, \sigma_{y*}^2) \propto -\frac{1}{2}\log(V_{y*}) - \frac{T-1}{2}\log(\sigma_{y*}^2) - \frac{1}{2}(\mathbf{W}_{\mathbf{y}*} - \gamma \mathbf{1}_T)'\boldsymbol{\Omega}_{\mathbf{y}*}^{-1}(\mathbf{W}_{\mathbf{y}*} - \gamma \mathbf{1}_T).$$

Combining this log density with the prior for γ gives:

$$\begin{aligned} \log p(\gamma \mid \mathbf{y}^*, \sigma_{y*}^2) &\propto \log p(\mathbf{W}_{\mathbf{y}*} \mid \mathbf{y}^*, \sigma_{y*}^2) + \log p(\gamma) \\ &\propto -\frac{1}{2}(\gamma(\mathbf{1}'_T \boldsymbol{\Omega}_{\mathbf{y}*}^{-1}\mathbf{1}_T + V_\gamma^{-1})\gamma - 2\gamma'(\mathbf{1}'_T \boldsymbol{\Omega}_{\mathbf{y}*}^{-1}(\mathbf{H}\mathbf{y}^* - \boldsymbol{\delta}_{\mathbf{y}*}) + V_\gamma^{-1}\gamma_0)). \end{aligned}$$

Therefore, $(\gamma \mid \mathbf{y}^*, \sigma_{y*}^2) \sim \mathcal{N}(\hat{\gamma}, D_\gamma)$, where

$$\begin{aligned} D_\gamma &= (\mathbf{1}'_T \boldsymbol{\Omega}_{\mathbf{y}*}^{-1}\mathbf{1}_T + V_\gamma^{-1})^{-1}, \\ \hat{\gamma} &= D_\gamma(\mathbf{1}'_T \boldsymbol{\Omega}_{\mathbf{y}*}^{-1}(\mathbf{H}\mathbf{y}^* - \boldsymbol{\delta}_{\mathbf{y}*}) + V_\gamma^{-1}\gamma_0). \end{aligned}$$

In the case of Step 4, the measurement Eq. (1) is stacked in a slightly different way:

$$\mathbf{y} = \mathbf{y}^* + \mathbf{U}\lambda + \boldsymbol{\epsilon}^{\mathbf{y}}, \tag{17}$$

where $\mathbf{U} = \mathrm{diag}((u_1 - u_1^*), \ldots, (u_T - u_T^*))$.

Using this representation, $(\mathbf{y} \mid \mathbf{y}^*, \mathbf{u}, \mathbf{u}^*, \lambda, \mathbf{h}) \sim \mathcal{N}(\mathbf{y}^* + \mathbf{U}\lambda, \boldsymbol{\Sigma})$, and hence the log sampling density is:

$$\log p(\mathbf{y} \mid \mathbf{y}^*, \mathbf{u}, \mathbf{u}^*, \lambda, \mathbf{h}) \propto -\frac{1}{2}\sum_{t=1}^{T} h_t - \frac{1}{2}(\mathbf{y} - \mathbf{y}^* - \mathbf{U}\lambda)'\boldsymbol{\Sigma}^{-1}(\mathbf{y} - \mathbf{y}^* - \mathbf{U}\lambda). \tag{18}$$

The next step is to stack the state equation for λ_t (4) in the following way:

$$\mathbf{H}\lambda = \tilde{\boldsymbol{\alpha}}_\lambda + \boldsymbol{\epsilon}^{\lambda}, \tag{19}$$

where $\tilde{\boldsymbol{\alpha}}_\lambda = (\lambda_0, 0, \ldots, 0)'$, $\boldsymbol{\epsilon}^\lambda \sim \mathcal{N}(\mathbf{0}, \boldsymbol{\Omega}_\lambda)$ and $\boldsymbol{\Omega}_\lambda = \mathrm{diag}(V_\lambda, \sigma_\lambda^2, \ldots, \sigma_\lambda^2)$.

It follows that $(\lambda \mid \sigma_\lambda^2) \sim \mathcal{N}(\boldsymbol{\alpha}_\lambda, (\mathbf{H}'\boldsymbol{\Omega}_\lambda^{-1}\mathbf{H})^{-1})$ and the log density is:

$$\log p(\lambda \mid \sigma_\lambda^2) \propto -\frac{1}{2}\log(V_\lambda) - \frac{T-1}{2}\log(\sigma_\lambda^2) - \frac{1}{2}(\lambda - \boldsymbol{\alpha}_\lambda)'\mathbf{H}'\boldsymbol{\Omega}_\lambda^{-1}\mathbf{H}(\lambda - \boldsymbol{\alpha}_\lambda). \tag{20}$$

Using Eqs. (18) and (20) to determine the conditional distribution:

$$\begin{aligned} &\log p(\lambda \mid \mathbf{y}, \mathbf{y}^*, \mathbf{u}, \mathbf{u}^*, \mathbf{h}, \sigma_\lambda^2) \\ &\propto \log p(\mathbf{y} \mid \mathbf{y}^*, \mathbf{u}, \mathbf{u}^*, \lambda, \mathbf{h}) + \log p(\lambda \mid \sigma_\lambda^2) \\ &\propto -\frac{1}{2}(\lambda'(\mathbf{U}'\boldsymbol{\Sigma}^{-1}\mathbf{U} + \mathbf{H}'\boldsymbol{\Omega}_\lambda^{-1}\mathbf{H})\lambda \\ &\qquad -2\lambda'(\mathbf{U}'\boldsymbol{\Sigma}^{-1}(\mathbf{y} - \mathbf{y}^*) + \mathbf{H}'\boldsymbol{\Omega}_\lambda^{-1}\mathbf{H}\boldsymbol{\alpha}_\lambda)). \end{aligned}$$

Therefore, $(\lambda \mid \mathbf{y}, \mathbf{y}^{*}, \mathbf{u}, \mathbf{u}^{*}, \mathbf{h}, \sigma_{\lambda}^{2}) \sim \mathcal{N}(\hat{\lambda}, \mathbf{D}_{\lambda})$, where

$$\mathbf{D}_{\lambda} = (\mathbf{U}'\boldsymbol{\Sigma}^{-1}\mathbf{U} + \mathbf{H}'\boldsymbol{\Omega}_{\lambda}^{-1}\mathbf{H})^{-1},$$
$$\hat{\lambda} = \mathbf{D}_{\lambda}(\mathbf{U}'\boldsymbol{\Sigma}^{-1}(\mathbf{y} - \mathbf{y}^{*}) + \mathbf{H}'\boldsymbol{\Omega}_{\lambda}^{-1}\mathbf{H}\boldsymbol{\alpha}_{\lambda}).$$

Again, given that $\boldsymbol{\Sigma}$, $\mathbf{H}$ and $\boldsymbol{\Omega}_{\lambda}$ are all band matrices, the precision-based algorithm in Chan and Jeliazkov (2009) can be used to sample λefficiently.

To implement Step 5, the auxiliary mixture sampler in Kim et al. (1998) is used to jointly sample the log-volatilities $\mathbf{h}$. The first step is to transform the measurement equation so that it is linear in the log-volatilities $\mathbf{h}$ (see, e.g. Chan and Hsiao, 2014):

$$\tilde{\mathbf{y}} = \mathbf{h} + \tilde{\epsilon}^{\mathbf{y}}, \tag{21}$$

where $\tilde{\mathbf{y}} = \log[(\mathbf{y} - \mathbf{y}^{*} - \boldsymbol{\Lambda}(\mathbf{u} - \mathbf{u}^{*}))^{2}]$ and $\tilde{\epsilon}^{\mathbf{y}} = \log[(\epsilon^{\mathbf{y}})^{2}]$. It follows that each element of $\tilde{\epsilon}^{y}$ has a log-χ_{1}^{2} distribution, which Kim et al. (1998) show can be approximated using a seven-component Gaussian mixture density with fixed parameters. By using mixture component indicators $s_t \in \{1, \ldots, 7\}$ for $t = 1,\ldots,T$, the measurement equation can be approximated by a conditionally linear Gaussian state space model.

Let the innovation be distributed as $(\tilde{\epsilon}^{\mathbf{y}} \mid \mathbf{s}) \sim \mathcal{N}(\boldsymbol{\mu}_{\mathbf{s}}, \boldsymbol{\Sigma}_{\mathbf{s}})$, with $\boldsymbol{\mu}_{\mathbf{s}}$ and $\boldsymbol{\Sigma}_{\mathbf{s}}$ being constant matrices that depend on $\mathbf{s} = (s_1, \ldots, s_T)'$, which are obtained from the Gaussian mixture approximation of the log-χ_{1}^{2} distribution. Therefore, the log sampling density is:

$$\log p(\tilde{\mathbf{y}} \mid \mathbf{h}, \boldsymbol{\mu}_{\mathbf{s}}, \boldsymbol{\Sigma}_{\mathbf{s}}) \propto -\frac{1}{2}\log|\boldsymbol{\Sigma}_{\mathbf{s}}| - \frac{1}{2}(\tilde{\mathbf{y}} - \mathbf{h} - \boldsymbol{\mu}_{\mathbf{s}})'\boldsymbol{\Sigma}_{\mathbf{s}}^{-1}(\tilde{\mathbf{y}} - \mathbf{h} - \boldsymbol{\mu}_{\mathbf{s}}). \tag{22}$$

The next step is to rewrite the transition equation for h_t (5) as:

$$\mathbf{H}\mathbf{h} = \tilde{\boldsymbol{\alpha}}_{\mathbf{h}} + \boldsymbol{\epsilon}^{\mathbf{h}}, \tag{23}$$

where $\tilde{\boldsymbol{\alpha}}_{\mathbf{h}} = (h_0, 0, \ldots, 0)'$, $\boldsymbol{\epsilon}^{\mathbf{h}} \sim \mathcal{N}(\mathbf{0}, \boldsymbol{\Omega}_{\mathbf{h}})$ and $\boldsymbol{\Omega}_{\mathbf{h}} = \mathrm{diag}(V_h, \sigma_h^2, \ldots, \sigma_h^2)$.

It follows that $(\mathbf{h} \mid \sigma_h^2) \sim \mathcal{N}(\boldsymbol{\alpha}_{\mathbf{h}}, (\mathbf{H}'\boldsymbol{\Omega}_{\mathbf{h}}^{-1}\mathbf{H})^{-1})$, where $\boldsymbol{\alpha}_{\mathbf{h}} = \mathbf{H}^{-1}\tilde{\boldsymbol{\alpha}}_{\mathbf{h}}$. Therefore, the log sampling density is:

$$\log p(\mathbf{h} \mid \sigma_h^2) \propto -\frac{1}{2}\log(V_h) - \frac{T-1}{2}\log(\sigma_h^2) - \frac{1}{2}(\mathbf{h} - \boldsymbol{\alpha}_{\mathbf{h}})'\mathbf{H}'\boldsymbol{\Omega}_{\mathbf{h}}^{-1}\mathbf{H}(\mathbf{h} - \boldsymbol{\alpha}_{\mathbf{h}}). \tag{24}$$

The conditional distribution can then be approximated using Eqs. (22) and (24):

$$\begin{aligned}
&\log p(\mathbf{h} \mid \mathbf{y}, \mathbf{y}^{*}, \mathbf{u}, \mathbf{u}^{*}, \lambda, \sigma_h^2)\\
&\quad\propto \log p(\tilde{\mathbf{y}} \mid \mathbf{h}, \boldsymbol{\mu}_{\mathbf{s}}, \boldsymbol{\Sigma}_{\mathbf{s}}) + \log p(\mathbf{h} \mid \sigma_h^2)\\
&\quad\propto -\frac{1}{2}(\mathbf{h}'(\boldsymbol{\Sigma}_{\mathbf{s}}^{-1} + \mathbf{H}'\boldsymbol{\Omega}_{\mathbf{h}}^{-1}\mathbf{H})\mathbf{h} - 2\mathbf{h}'(\boldsymbol{\Sigma}_{\mathbf{s}}^{-1}(\tilde{\mathbf{y}} - \boldsymbol{\mu}_{\mathbf{s}}) + \mathbf{H}'\boldsymbol{\Omega}_{\mathbf{h}}^{-1}\mathbf{H}\boldsymbol{\alpha}_{\mathbf{h}})).
\end{aligned}$$

Therefore, the precision sampler of Chan and Jeliazkov (2009) can be used to sample from $(\mathbf{h} \mid \mathbf{y}, \mathbf{y}^{*}, \mathbf{u}, \mathbf{u}^{*}, \lambda, \sigma_h^2) \sim \mathcal{N}(\hat{\mathbf{h}}, \mathbf{D}_{\mathbf{h}})$, where

$$\mathbf{D}_{\mathbf{h}} = (\boldsymbol{\Sigma}_{\mathbf{s}}^{-1} + \mathbf{H}'\boldsymbol{\Omega}_{\mathbf{h}}^{-1}\mathbf{H})^{-1}, \quad \hat{\mathbf{h}} = \mathbf{D}_{\mathbf{h}}(\boldsymbol{\Sigma}_{\mathbf{s}}^{-1}(\tilde{\mathbf{y}} - \boldsymbol{\mu}_{\mathbf{s}}) + \mathbf{H}'\boldsymbol{\Omega}_{\mathbf{h}}^{-1}\mathbf{H}\boldsymbol{\alpha}_{\mathbf{h}}).$$

In the case of Step 6, the AR(2) process in Eq. (3) can be rewritten in the following form, given the assumption that $\varepsilon_0^u = \varepsilon_{-1}^u = 0$ and $\boldsymbol{\epsilon}^{\mathbf{u}}$ is known given $\mathbf{u}$ and $\mathbf{u}^{*}$:

$$\boldsymbol{\epsilon}^{\mathbf{u}} = \mathbf{X}\boldsymbol{\rho} + \boldsymbol{\eta}, \tag{25}$$

where $\boldsymbol{\eta} \sim \mathcal{N}(\mathbf{0}, \mathbf{I}_T\sigma_u^2)$, $\boldsymbol{\rho} = (\rho_1, \rho_2)'$ and

$$\mathbf{X} = \begin{pmatrix} 0 & 0 \\ \varepsilon_1^u & 0 \\ \varepsilon_2^u & \varepsilon_1^u \\ \varepsilon_3^u & \varepsilon_2^u \\ \vdots & \vdots \\ \varepsilon_{T-1}^u & \varepsilon_{T-2}^u \end{pmatrix}.$$

Therefore, it follows that $(\boldsymbol{\epsilon}^{\mathbf{u}} \mid \boldsymbol{\rho}, \sigma_u^2) \sim \mathcal{N}(\mathbf{X}\boldsymbol{\rho}, \mathbf{I}_T\sigma_u^2)$ and the log density is:

$$\log p(\boldsymbol{\epsilon}^{\mathbf{u}} \mid \boldsymbol{\rho}, \sigma_u^2) \propto -\frac{T}{2}\log(\sigma_u^2) - \frac{1}{2\sigma_u^2}(\boldsymbol{\epsilon}^{\mathbf{u}} - \mathbf{X}\boldsymbol{\rho})'(\boldsymbol{\epsilon}^{\mathbf{u}} - \mathbf{X}\boldsymbol{\rho}). \tag{26}$$

Combining this log density with the prior for $\boldsymbol{\rho}$ gives:

$$\begin{aligned}
&\log p(\boldsymbol{\rho} \mid \mathbf{u}, \mathbf{u}^{*}, \sigma_u^2)\\
&\quad\propto \log p(\boldsymbol{\epsilon}^{\mathbf{u}} \mid \boldsymbol{\rho}, \sigma_u^2) + \log p(\boldsymbol{\rho})\\
&\quad\propto -\frac{1}{2}(\boldsymbol{\rho}'(\mathbf{X}'\mathbf{X}/\sigma_u^2 + \mathbf{V}_{\rho}^{-1})\boldsymbol{\rho} - 2\boldsymbol{\rho}'(\mathbf{X}'\boldsymbol{\epsilon}^{\mathbf{u}}/\sigma_u^2 + \mathbf{V}_{\rho}^{-1}\boldsymbol{\rho}_{\mathbf{0}})).
\end{aligned}$$

Therefore, $(\boldsymbol{\rho} \mid \mathbf{u}, \mathbf{u}^{*}, \sigma_u^2) \sim \mathcal{N}(\hat{\boldsymbol{\rho}}, \mathbf{D}_{\rho})$, where

$$\mathbf{D}_{\rho} = (\mathbf{X}'\mathbf{X}/\sigma_u^2 + \mathbf{V}_{\rho}^{-1})^{-1}, \quad \hat{\boldsymbol{\rho}} = \mathbf{D}_{\rho}(\mathbf{X}'\boldsymbol{\epsilon}^{\mathbf{u}}/\sigma_u^2 + \mathbf{V}_{\rho}^{-1}\boldsymbol{\rho}_{\mathbf{0}}).$$

To implement Step 7, the log conditional density is derived using the non-matrix form of the density (26) and the prior for σ_u^2 as follows:

$$\log p(\sigma_u^2 \mid \boldsymbol{\rho}, \mathbf{u}, \mathbf{u}^*) \propto \log p(\boldsymbol{\epsilon}^{\mathbf{u}} \mid \boldsymbol{\rho}, \sigma_u^2) + \log p(\sigma_u^2)$$
$$\propto \left(-\frac{T}{2} - \nu_u - 1\right)\log(\sigma_u^2) - \frac{1}{\sigma_u^2}\left(S_u + \frac{\sum_{t=1}^{T}(\epsilon_t^u - \rho_1\epsilon_{t-1}^u - \rho_2\epsilon_{t-2}^u)^2}{2}\right).$$

Therefore, $(\sigma_u^2 \mid \boldsymbol{\rho}, \mathbf{u}, \mathbf{u}^*) \sim \mathcal{IG}\left(\frac{T}{2} + \nu_u, S_u + \frac{\sum_{t=1}^{T}(\epsilon_t^u - \rho_1\epsilon_{t-1}^u - \rho_2\epsilon_{t-2}^u)^2}{2}\right)$.

Step 8 is implemented in a similar manner, with the log conditional density derived as:

$$\log p(\sigma_\lambda^2 \mid \boldsymbol{\lambda}) \propto \log p(\boldsymbol{\lambda} \mid \sigma_\lambda^2) + \log p(\sigma_\lambda^2)$$
$$\propto \left(-\frac{T-1}{2} - \nu_\lambda - 1\right)\log(\sigma_\lambda^2) - \frac{1}{\sigma_\lambda^2}\left(S_\lambda + \frac{\sum_{t=2}^{T}(\lambda_t - \lambda_{t-1})^2}{2}\right).$$

Therefore, $(\sigma_\lambda^2 \mid \boldsymbol{\lambda}) \sim \mathcal{IG}\left(\frac{T-1}{2} + \nu_\lambda, S_\lambda + \frac{\sum_{t=2}^{T}(\lambda_t - \lambda_{t-1})^2}{2}\right)$.

Similarly, for Step 9, the log conditional density is derived as:

$$\log p(\sigma_h^2 \mid \mathbf{h}) \propto \log p(\mathbf{h} \mid \sigma_h^2) + \log p(\sigma_h^2)$$
$$\propto \left(-\frac{T-1}{2} - \nu_h - 1\right)\log(\sigma_h^2) - \frac{1}{\sigma_h^2}\left(S_h + \frac{\sum_{t=2}^{T}(h_t - h_{t-1})^2}{2}\right).$$

Therefore, $(\sigma_h^2 \mid \mathbf{h}) \sim \mathcal{IG}\left(\frac{T-1}{2} + \nu_h, S_h + \frac{\sum_{t=2}^{T}(h_t - h_{t-1})^2}{2}\right)$.

For Step 10, the log conditional density is:

$$\log p(\sigma_{y*}^2 \mid \mathbf{y}^*) \propto \log p(\mathbf{y}^* \mid \sigma_{y*}^2) + \log p(\sigma_{y*}^2)$$
$$\propto \left(-\frac{T-1}{2} - \nu_{y*} - 1\right)\log(\sigma_{y*}^2) - \frac{1}{\sigma_{y*}^2}\left(S_{y*} + \frac{\sum_{t=2}^{T}(y_t^* - \gamma - y_{t-1}^*)^2}{2}\right).$$

Therefore, $(\sigma_{y*}^2 \mid \mathbf{y}^*) \sim \mathcal{IG}\left(\frac{T-1}{2} + \nu_{y*}, S_{y*} + \frac{\sum_{t=2}^{T}(y_t^* - \gamma - y_{t-1}^*)^2}{2}\right)$.

Finally, to implement Step 11, the log conditional density is derived as follows:

$$\log p(\sigma_{u*}^2 \mid \mathbf{u}^*) \propto \log p(\mathbf{u}^* \mid \sigma_{u*}^2) + \log p(\sigma_{u*}^2)$$
$$\propto \left(-\frac{T-1}{2} - \nu_{u*} - 1\right)\log(\sigma_{u*}^2) - \frac{1}{\sigma_{u*}^2}\left(S_{u*} + \frac{\sum_{t=2}^{T}(u_t^* - u_{t-1}^*)^2}{2}\right).$$

Therefore, $(\sigma_{u*}^2 \mid \mathbf{u}^*) \sim \mathcal{IG}\left(\frac{T-1}{2} + \nu_{u*}, S_{u*} + \frac{\sum_{t=2}^{T}(u_t^* - u_{t-1}^*)^2}{2}\right)$.

References

Arias, A., Hansen, G., Ohanian, L., 2007. Why have business cycle fluctuations become less volatile? Econ. Theory 32 (1), 43–58.
Ball, L., Leigh, D., Loungani, P., 2013. Okun's Law: Fit at Fifty?. National Bureau of Economic Research.
Basu, D., Foley, D., 2013. Dynamics of output and employment in the us economy. Camb. J. Econ. 37 (5), 1077–1106.
Beaton, K., 2010. Time variation in Okun's law: A Canada and US comparison, Bank of Canada Working Paper.
Benati, L. Mumtaz, H. 2007. US evolving macroeconomic dynamics: A structural investigation, Working paper 746, European Central Bank.
Berger, T., Everaert, G., Vierke, H., 2016. Testing for time variation in an unobserved components model for the US economy. J. Econ. Dyn. Control 69, 179–208.
Boeri, T., Garibaldi, P., Moen, E., 2013. Financial shocks and labor: facts and theories. IMF Econ. Rev. 61 (4), 631–663.
Boivin, J., Giannoni, M., 2006. Has monetary policy become more effective? Rev. Econ. Stat. 88 (3), 445–462.
Calvo, G., Coricelli, F., Ottonello, P., 2013. Jobless Recoveries During Financial Crises: Is Inflation the Way Out?. National Bureau of Economic Research.
Canova, F., 1998. Detrending and business cycle facts. J. Monet. Econ. 41 (3), 475–512.
Chan, J., 2015. The stochastic volatility in mean model with time-varying parameters: an application to inflation modeling. J. Bus. Econ. Stat., (Forthcoming).
Chan, J., Hsiao, C., 2014. Estimation of stochastic volatility models with heavy tails and serial dependence. In: Jeliazkov, I., Yang, X.-S. (Eds.), Bayesian Inference in the Social Sciences. John Wiley & Sons, Hoboken.
Chan, J., Jeliazkov, I., 2009. Efficient simulation and integrated likelihood estimation in state space models. Int. J. Math. Model. Numer. Optim. 1 (1), 101–120.
Chan, J., Koop, G., Potter, S., 2016. A bounded model of time variation in trend inflation, NAIRU and the Phillips curve. J. Appl. Econ. 31 (3), 551–565.
Chen, J., Kannan, P., Trehan, B. Loungani, P., 2012. New evidence on cyclical and structural sources of unemployment, IMF Working Paper.
Cheng, K., Durmaz, N., Kim, H., Stern, M., 2012. Hysteresis vs. natural rate of US unemployment. Econ. Model. 29 (2), 428–434.
Chinn, M., Ferrara, L., Mignon, V., 2014. Explaining US employment growth after the Great Recession. J. Macroecon. 42, 118–129.
Clarida, R., Galí, J., Gertler, M., 2000. Monetary policy rules and macroeconomic

stability: evidence and some theory. Q. J. Econ. 115 (1), 147–180.
Cogley, T., Nason, J., 1995. Effects of the Hodrick-Prescott filter on trend and difference stationary time series: implications for business cycle research. J. Econ. Dyn. Control 19 (1), 253–278.
Cogley, T., Sargent, T., 2005. Drifts and volatilities: monetary policies and outcomes in the post WWII US. Rev. Econ. Dyn. 8 (2), 262–302.
Cuaresma, J., 2003. Okun's law revisited. Oxf. Bull. Econ. Stat. 65 (4), 439–451.
Daly, M., Hobijn, B., Sahin, A., Valletta, R. et al. 2011. A rising natural rate of unemployment: Transitory or permanent?'. Tinbergen Institute Discussion Paper.
Dixon, R., Lim, G., van Ours, J., 2017. Revisiting the Okun relationship. Appl. Econ. 49 (28), 2749–2765.
Farber, H., 2012. Unemployment in the Great Recession: did the housing market crisis prevent the unemployed from moving to take jobs? Am. Econ. Rev. 102 (3), 520–525.
Galí, J., Gambetti, L., 2009. On the sources of the Great moderation. Am. Econ. J.: Macroecon. 1 (1), 26–57.
Galí, J., Smets, F., Wouters, R., 2012. Slow recoveries: a structural interpretation. J. Money, Credit Bank. 44 (s2), 9–30.
Gambetti, L., Pappa, E., Canova, F., 2008. The structural dynamics of US output and inflation: What explains the changes? J. Money, Credit Bank. 40 (2–3), 369–388.
Gordon, R., 2010. The demise of Okun's law and of procyclical fluctuations in conventional and unconventional measures of productivity, For Presentation at NBER Summer Institute, PRBB Resarch Meeting.
Guisinger, A., Hernandez-Murillo, R., Owyang, M. Sinclair, T., 2015. A state-level analysis of Okun's law, Federal Reserve Bank of St. Louis Working Paper.
Hall, R., 2017. The anatomy of stagnation in a modern economy. Economica 84 (333), 1–15.
Holmes, M., Silverstone, B., 2006. Okun's law, asymmetries and jobless recoveries in the United States: a Markov-switching approach. Econ. Lett. 92 (2), 293–299.
Huang, H.-C., Lin, S.-C., 2008. Smooth-time-varying Okun's coefficients. Econ. Model. 25 (2), 363–375.
Justiniano, A., Primiceri, G., 2008. The time-varying volatility of macroeconomic fluctuations. Am. Econ. Rev. 98 (3), 604–641.
Kaufman, R., 1988. An international comparison of Okun's laws. J. Comp. Econ. 12 (2), 182–203.
Kim, S., Shepherd, N., Chib, S., 1998. Stochastic volatility: likelihood inference and comparison with ARCH models. Rev. Econ. Stud. 65 (3), 361–393.
King, R., Rebelo, S., 1993. Low frequency filtering and real business cycles. J. Econ. Dyn. Control 17 (1), 207–231.
Koop, G., Leon-Gonzalez, R., Strachan, R., 2010. Dynamic probabilities of restrictions in state space models: an application to the Phillips curve. J. Bus. Econ. Stat. 28 (3), 370–379.
Lazear, E., Spletzer, J., 2012. The United States labor market: status quo or a new normal?. National Bureau of Economic Research.
Lee, J., 2000. The robustness of Okun's law: evidence from OECD countries. J. Macroecon. 22 (2), 331–356.
Lubik, T., Schorfheide, F., 2004. Testing for indeterminacy: an application to US monetary policy. Am. Econ. Rev. 94 (1), 190–217.
Marques, A., Lima, G., Troster, V., 2017. Unemployment persistence in OECD countries after the Great Recession. Econ. Model. 64, 105–116.
McCausland, W., Miller, S., Pelletier, D., 2011. Simulation smoothing for state-space models: a computational efficiency analysis. Comput. Stat. Data Anal. 55 (1), 199–212.
Moosa, I., 1997. A cross-country comparison of Okun's coefficient. J. Comp. Econ. 24 (3), 335–356.
Okun, A., 1962. Potential GNP: its measurement and significance. Am. Stat. Assoc., Proc. Bus. Econ. Stat. Sect., 98–104.
Prachowny, M., 1993. Okun's law: theoretical foundations and revised estimates. Rev. Econ. Stat. 75 (2), 331–336.
Primiceri, G., 2005. Time varying structural vector autoregressions and monetary policy. Rev. Econ. Stud. 72 (3), 821–852.
Silvapulle, P., Moosa, I., Silvapulle, M., 2004. Asymmetry in Okun's law. Can. J. Econ. 37 (2), 353–374.
Sims, C., Zha, T., 2006. Were there regime switches in US monetary policy? Am. Econ. Rev. 96 (1), 54–81.
Sögner, L., 2001. Okun's law: does the Austrian unemployment-GDP relationship exhibit structural breaks? Empir. Econ. 26 (3), 553–564.
Sögner, L., Stiassny, A., 2002. An analysis on the structural stability of Okun's law: a cross-country study. Appl. Econ. 34 (14), 1775–1787.
Stock, J., Watson, M., 2012. Disentangling the channels of the 2007–2009 recession. Natl. Bur. Econ. Res..
Valadkhani, A., Smyth, R., 2015. Switching and asymmetric behaviour of the Okun coefficient in the US: evidence for the 1948-2015 period. Econ. Model. 50, 281–290.
Wang, X., Huang, H., 2017. Okun's law revisited: a threshold in regression quantiles approach. Appl. Econ. Lett., (Forthcoming).
Weber, C., 1995. Cyclical output, cyclical unemployment, and Okun's coefficient: a new approach. J. Appl. Econ. 10 (4), 433–445.
Zanin, L., Marra, G., 2012. Rolling regression versus time-varying coefficient modelling: an empirical investigation of the Okun's law in some euro area countries. Bull. Econ. Res. 64 (1), 91–108.